

Original Articles

Combined microdrop generation and microdiffraction for biopolymer hydration experiments

C. Riekkel, M. Burghammer, D. Flot and M. Rössle

European Synchrotron Radiation Facility, B.P. 220, F-38043 Grenoble Cedex, France

Received 5th January 2004; accepted in revised form 16th March 2004

ABSTRACT

The article discusses instrumentation developed at the ESRF ID13 beamline for the study of rapid biopolymer hydration reactions. An introduction into currently available optics and sample environments is provided and the use of a 0.7 μm beam is demonstrated for SAXS/WAXS patterns recorded from a starch granule. An inkjet system is described, which allows hydration of biopolymers locally with about 50 μm diameter water droplets. The application of this system to β -chitin hydration is described and an outlook on future possibilities, including rapid droplet mixing reactions, is given.

Introduction

The microstructural properties of biopolymers depend often on their water content and it is therefore important to control the hydration level in X-ray scattering experiments. The high flux density of synchrotron radiation (SR) microbeam experiments [1] is particularly challenging for in-situ experiments on hydrated biopolymers due to the risk of secondary radiation damage as for protein crystals [2]. Thus the crystallinity in hydrated potato starch granules was found to disappear at room temperature for X-ray doses above 5 photons nm^{-3} , which limited data collection times in SR-microdiffraction experiments to a few seconds per pattern [3]. An experimental challenge is therefore to conceive techniques, which allow investigating the local hydration kinetics of a biopolymeric sample - such as a starch granule - by SR-microdiffraction. We are currently exploring inkjet-systems [4] for such applications at the ESRF microfocuss beamline (ID13).

Microdrops (or droplets) of water or other liquids can be generated by various inkjet-systems [4]. The minimum droplet size can reach the μm -scale. Water droplets of 30-50 μm diameters can be easily produced by drop-on-demand systems [4]. For such systems, droplets are not heated during ejection and can carry proteins or even biological objects without damage. A useful property of water droplets is the domination of the surface energy (E_{sur}) with respect to kinetic energy (E_{kin}) for droplet diameters of about 100 μm or smaller: (Fig.1.A)

$$E_{\text{kin}}/E_{\text{sur}} = (1/6 \rho/\sigma)v^2 r \quad (1)$$

with the parameters: r : radius, v : velocity, ρ : density, σ : surface tension. For droplets with $r=25 \mu\text{m}$, $\rho=1 \text{ g/cm}^3$, $\sigma=0.073 \text{ N/m}$ and $v=2.5 \text{ m/sec}$ a value of $E_{\text{kin}}/E_{\text{sur}} \approx 0.36$ is calculated. This implies that the droplets will not splash when hitting a target. The surface properties of the fibre will not play a role in this impact phase [5]. The high position definition of droplets is shown in Fig.1.B where a single droplet was dispensed on a 12 μm diameter Kevlar fibre. The hydrophobic fibre surface

results in this case in a high contact angle and the water droplet will disappear upon evaporation. For more hydrophilic surfaces spreading of the droplet will occur depending on the contact angle [5]. In addition volume hydration as observed for β -chitin is possible [6], which could be used for locally hydrating a fibre.

The aim of the present report is to give an update on the current ID13 beamline instrumentation, the technical aspects of microdrop experiments and future experimental possibilities. As a practical case, the hydration of the polysaccharide β -chitin will be discussed.

Experimental methods

Synchrotron radiation set-ups used at the ID13 beamline are located in two experimental hutches: EH-1/EH-2 [7]. EH-1 houses a microgoniometer, which is used for microcrystallography and fibre diffraction [8]. The minimum beam size is currently 5 μm for a 0.2 mrad divergence based on a condensing ellipsoidal mirror and a defining aperture. EH-2 houses a scanning small-angle/wide-angle X-ray scattering (SAXS/WAXS) set-up [7, 9]. A beam size of 5 μm for a 0.2 mrad divergence is obtained by a combination of Kirkpatrick-Baez (KB) mirror [7, 10] and defining/guard apertures. The typically available SAXS-resolution is shown in Fig.2.A for a pair of dry rats tail collagen fibres held at right angles. A high demagnification KB-mirror system [11] has been recently commissioned for sub- μm beam applications. The free space available between the optics and the sample is $\approx 16\text{mm}$, which provides more space for sample environments as compared to glass capillary optics [1] and allows to introduce guard apertures for optimizing SAXS signals [9]. A beam size of 0.7 μm for a divergence of $\approx 0.3\text{mrad}$ has been reached with this set-up. The SAXS-resolution currently available is shown in Fig. 2.B for a collagen fibre. This set-up will provide new opportunities for soft condensed matter and biopolymer experiments. Thus Fig. 3 shows a scan across an about 70 μm diameter hydrated potato starch granule with 5 μm step increment and 100 ms exposure time using a MAR CCD detector (see below). The grain was kept in water filled

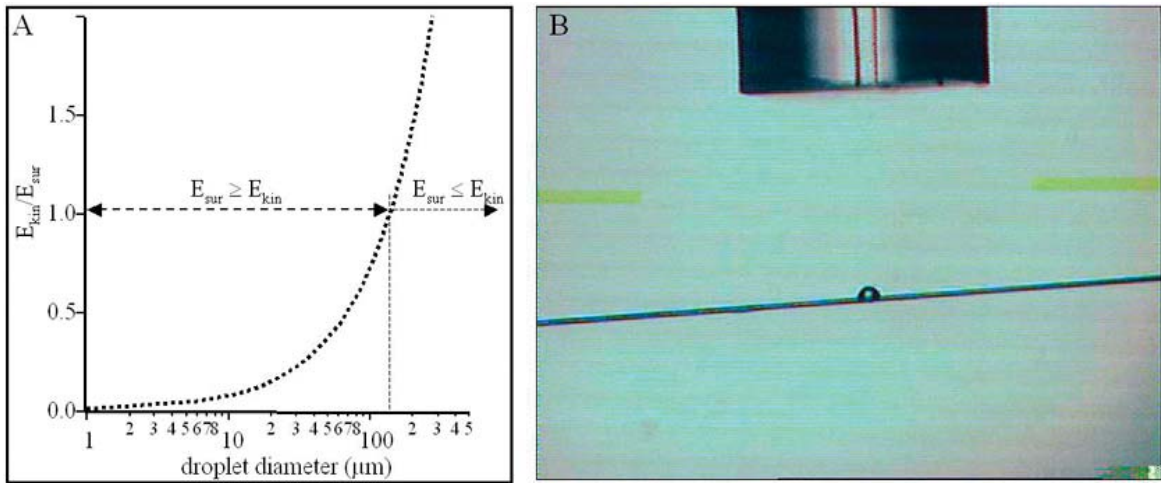


Figure 1. A: variation of ratio of surface energy (E_{sur}) and kinetic energy (E_{kin}) as a function of the size of a spherical water droplet; B: a 50 μm diameter water droplet has been ejected from the glass capillary head of the dispensing system and has remained attached to the surface of a 12 μm diameter Kevlar fibre.

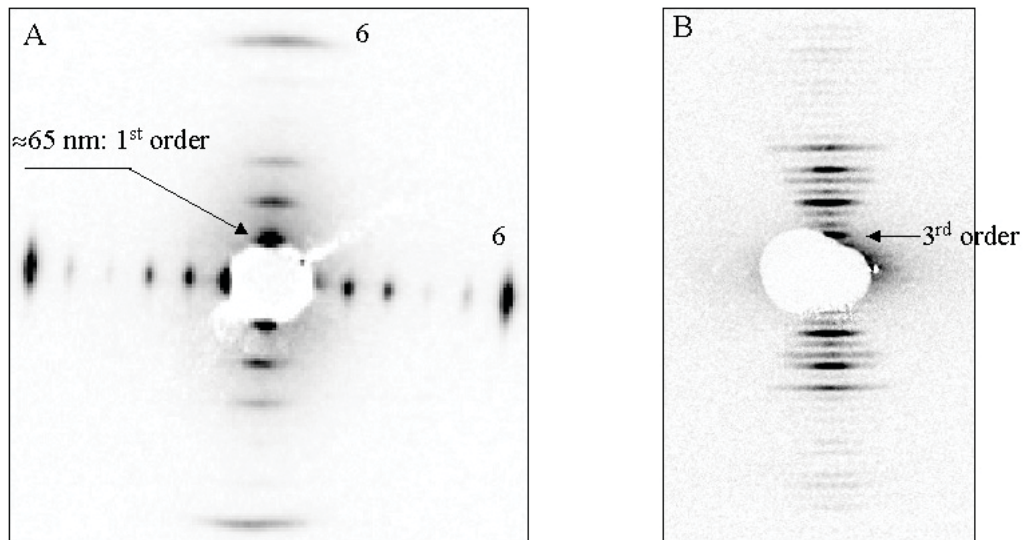


Figure 2. A: SAXS pattern of a cross of dry rats tail collagen fibres recorded with 5 μm beam; B: SAXS pattern of same collagen fibre recorded with a 0.7 μm beam.

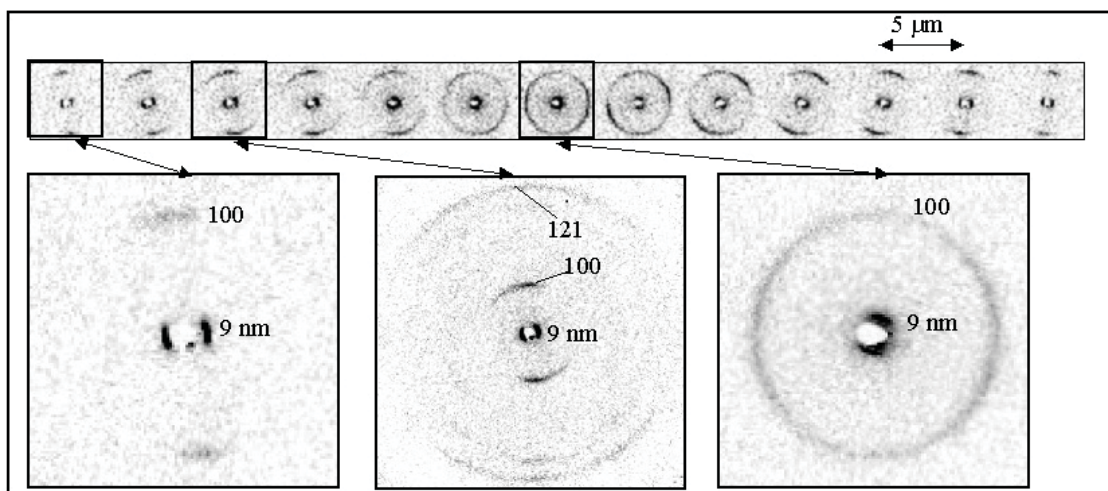


Figure 3. SAXS/WAXS patterns recorded with a 0.7 μm beam for a step-scan with 5 μm increment across a hydrated potato starch granule. The upper display range of the patterns in the sequence is limited to the 100 reflection. Selected patterns are shown in more detail.

borosilicate capillary. The patterns correspond to the starch B structure [12]. The combined SAXS/WAXS experiment shows for the first time for a single granule the coexistence of the meridional ($d \approx 9$ nm) and the equatorial ($100: d = 1.5_5$ nm) reflections [13-15]. The meridional reflection is due to the lamellar morphology of the semicrystalline material [16, 17] while the equatorial reflection is due to the incorporation of water into the lattice sites of the starch structure [12, 18, 19].

Experiments on biopolymers in EH-2 are usually performed with a monochromatic beam of $\lambda = 0.097$ nm, which is close to the optimum flux of an in-vacuum undulator with 18 mm period [7, 10]. Diffraction patterns reported below have been recorded using a MAR-CCD (2Kx2K; 16 bit readout). By binning to 512x512 pixels the readout time per frame can be reduced to 3.5 sec. The set-up is shown schematically in Fig. 4.

The microdrop generator is based on a glass capillary mounted concentrically in a piezoelectric actuator. (Microdrop, Norderstedt, Germany). This system has been used until now at the microgoniometer [8] but is in principle portable. The droplet diameter is defined by the capillary exit to about 50 μ m. A droplet frequency of a few Hz allows the maintenance of a constant liquid supply at the sample position. The control unit of the system is triggered by a TTL signal from a VME frequency generator board. Software control is possible through a SPEC interface (Certified Scientific Software). The droplet can be visualized by stroboscopic illumination triggered by the microdrop electronics. (Fig. 4)

Applications and perspectives

β -Chitin

The monoclinic β -chitin structure is composed of β -chitin microfibrils, packed parallel into flat ribbons, which form sheets by hydrogen-bonding (Fig. 5.A) [20, 21]. Water can be intercalated between these sheets to form a monohydrate and a dihydrate phases, which can be reversibly transformed [22]. The intercalation increases basically only the size of the b-axis.

The β -chitin material used came from *Birsteinia* tubes, which are the habitat of the deep-sea worm *Pogonophora* (Fig. 5.B,C). Flat ribbons of parallel chitin microfibrils, which are embedded in a protein matrix, form the tube wall. Dry tube fragments were mounted on glass tips, glued to standard crystallography sample holders and transferred to the microgoniometer. A 100 ms diffraction pattern shows a weak fibre texture (Fig. 5.D) in agreement with the fibrillar morphology (Fig. 5.C).

For the hydration reaction water droplets of 50 μ m diameter (=65 pl) were dispensed with a frequency of 10 droplets per second. Short exposure time (100 msec) and changing the probing position of the 5 μ m beam by 8 μ m steps in a systematic way, allowed reduction of secondary radiation damage. A time sequence of 1D-diffraction patterns is shown in Fig. 6 [6]. The reflection positions show that the anhydrous phase is transformed into the dihydrate phase via an intermediary diffuse monohydrate phase. In contrast to the steady state analysis [23], the kinetic data suggest that the monohydrate phase is a highly disordered nucleation phase for the dihydrate phase. One should also note that the total water

consumption is only about 100 nl, which is very useful when working with precious (e.g. protein containing) solutions.

Perspectives

Faster processes could be investigated provided that the onset of hydration can be better defined. Thus for a droplet with 2 m/sec speed the flight time from the microdrop capillary exit to the -say- 200 μ m distant sample surface is only 0.1 msec. By synchronizing the droplet ejection with the data acquisition system one could therefore reach ms- or sub-ms time-scales. Instead of solid/liquid reactions one could also investigate liquid/liquid reactions involving conformational changes in solution (e.g. proteins) or nucleation/precipitation reactions. Fast conformational changes have been investigated on the ms-scale with microfluidic devices using a lamellar flow geometry [24-26] while crossed-droplet experiments would correspond to turbulent mixing processes. For such applications the triggering pulse from the microdrop electronics has to be synchronized with the data acquisition system in order to stroboscopically observe droplets at a selected position after ejection from the capillary nozzle (Fig. 7). This is possible for the ID13 *Frelon* CCD-camera (current parameters: 2Kx2K pixels, 14 bit readout, readout frequency: 10 Hz), which has an image intensifier stage based on a *Proxitronic* microchannel plate (MCP) (Fig. 4). The MCP can be operated in a triggered gated mode with 100 ns minimum gating time [28]. Mixing liquids by continuous stream methods are further possibilities, which have not been explored until now [4].

Acknowledgements

The authors wish to thank H. Chanzy, CERMAV-Grenoble who kindly provided the β -chitin material. I. Snigireva (ESRF) recorded the SEM pictures. H. Gonzalez, L. Lardiere, J. Meyer and C. Ponchut provided technical support.

References

- [1] Riekkel, C. (2000) New avenues in X-ray microbeam experiments. *Rep. Prog. Phys.*, **63**, 233-262.
- [2] Teng, T. and Moffat, K. (2000) Primary radiation damage of protein crystals by intense synchrotron X-ray beam. *J. Synchrotron Rad.*, **7**, 313-317.
- [3] Buléon, A., Pontoire, B., Riekkel, C., Chanzy, H., Helbert, W. and Vuong, R. (1997) Crystalline Ultrastructure of starch granules revealed by synchrotron radiation microdiffraction mapping. *Macromolecules*, **30**, 3952-3954.
- [4] Lee, E.R. (2003) in *Microdrop Generation*. Nano- and Microscience, Engineering, Technology, and Medicine Series, S.E. Lyshevski, Editor, Boca Raton: CRC Press.
- [5] Maier, C., a.d. Wiesche, S., and Hofer, E.P. (2000) Impact of Microdrops on Solid Surfaces for DNA-Synthesis. in *2000 International Conference on Modeling and Simulation of Microsystems*. Nano Science & Technology Institute, **3**, 586-589.
- [6] Rössle, M., Flot, D., Engel, J., Riekkel, C. and Chanzy, H. (2003) Fast intra-crystalline hydration of β -chitin revealed by a combined microdrop generation and on-line synchrotron radiation microdiffraction. *Biomacromolecules*, **4**, 981-986.
- [7] Riekkel, C. (2002) Current limits of X-ray microdiffraction in soft condensed matter experiments. *Fibre Diffraction Review*, **10**, 11-18.

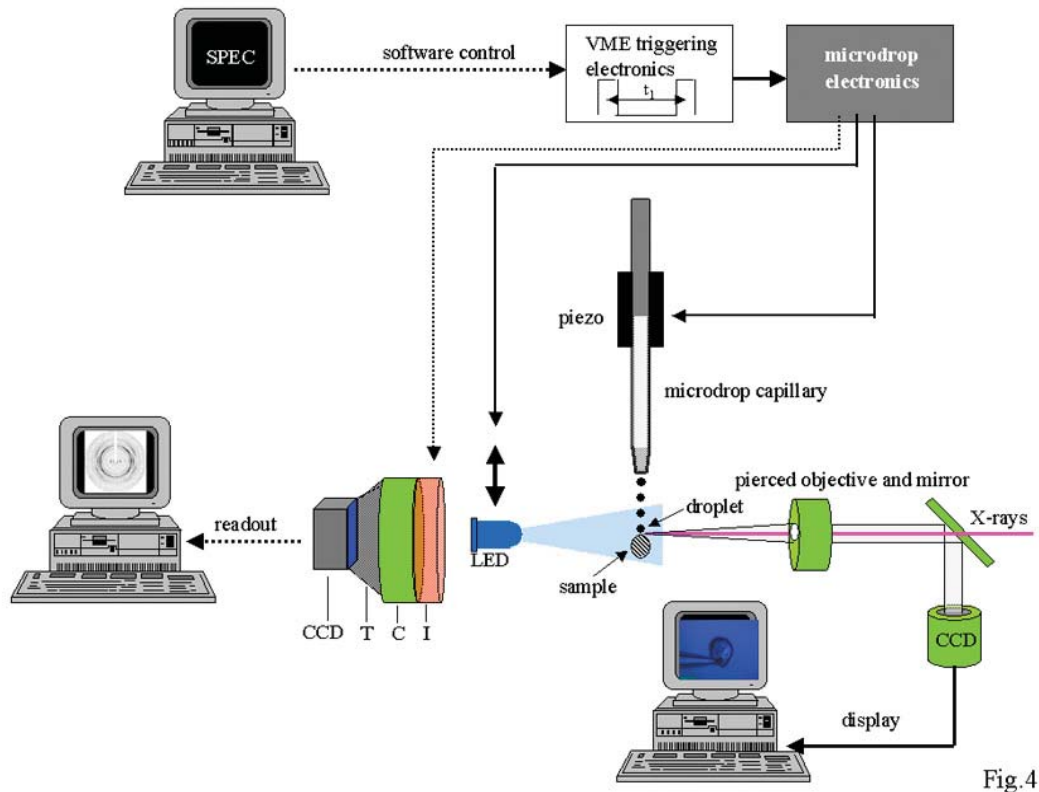


Fig.4

Figure 4. Schematic design of data acquisition system used for microdrop experiments. The microdrop electronics is controlled through a VME board by a UNIX workstation with SPEC software. The triggering signal from the microdrop electronics triggers the microdrop-piezo and the LED for stroboscopic illumination. The detector is composed of a converter screen (C), a fibre-optics taper (T) and a CCD. For special applications, an image intensifier stage with converter screen (I) is coupled with a CCD. The trigger signal from the microdrop electronics triggers the intensifier stroboscopically. The sample observation system corresponds to the microgoniometer [8].

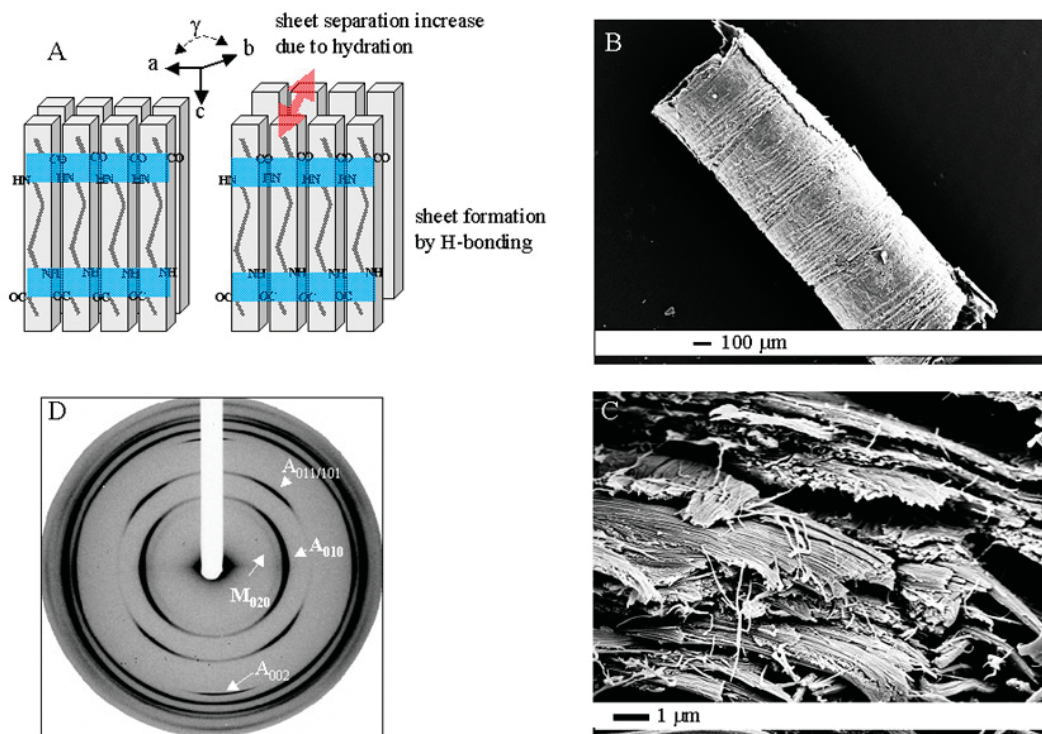


Figure 5. A: schematic structure of monoclinic β -chitin: P21: $a=0.485$, $b=0.926$, $c=1.038$, $\gamma=97.50$ [20]. The polymeric chains are depicted as slabs, which form sheets through hydrogen-bonding interactions. Hydration increases the b -axis via the sheet-separation; B: scanning electron microscopy image (SEM) of dry *Birsteinia* tube; C: higher resolution SEM image of the tube wall; D: diffraction pattern from the tube wall recorded in 100 ms using a $5 \mu\text{m}$ beam. The pattern shows principally reflections of anhydrous β -chitin (A) and a weak fraction of monohydrate phase (M).

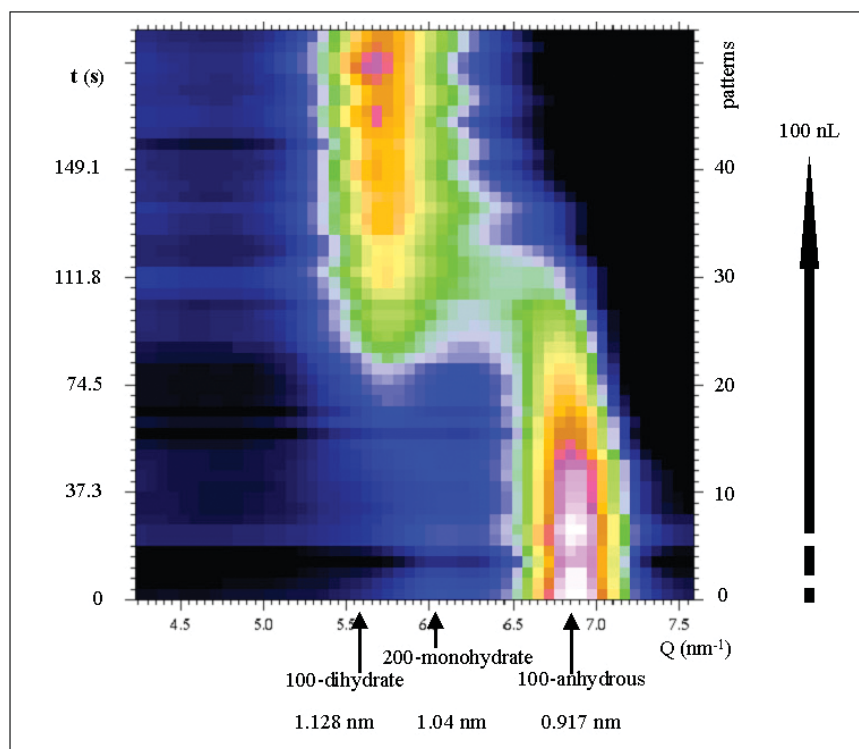


Figure 6. Variation of 1D-diffraction patterns during β -chitin hydration. The reported reflection positions of $0k0$ reflections corresponding to the layer-separation of β -chitin [20, 22], monohydrate[20] and dihydrate[27] phases have been indicated (adapted from Rössle *et al.*, [6]).

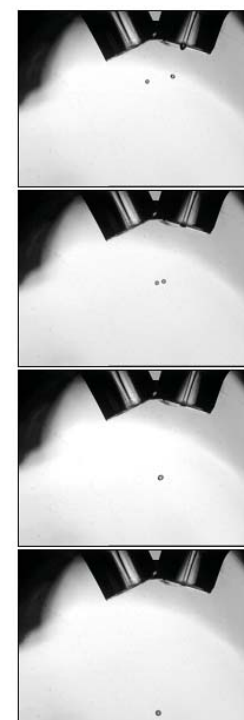


Figure 7. Crossed droplet experiment based on two microdrop capillary heads. The stroboscopic images show the ejection of two droplets and their fusion into a single droplet.

[8] Riekkel, C. (2003) Recent developments in microdiffraction on protein crystals. *J. Synchr. Rad.*, **11**, 4-6.
 [9] Riekkel, C., Burghammer, M. and Müller, M. (2000) Microbeam small-angle scattering experiments and their combination with microdiffraction. *J. Appl. Cryst.*, **33**, 421-423.
 [10] Riekkel, C. and Vincze, L. (2003) Status and perspectives of capillary optics at a third-generation synchrotron radiation source. *X-ray spectrometry*, **32**, 208-214.
 [11] Hignette, O., Rostaing, G., Cloetens, P., Rommeveaux, A., Ludwig, W. and Freund, A. (2001) Submicron focusing of hard X-rays with reflecting surfaces at the ESRF. in *SPIE Conference Proceedings 4499*. I. McNulty, Editor, San Diego, 105-116.
 [12] Sarko, A. and Wu, H.C.H. (1978) The crystal structure of A,B and C polymorphs of amylose and starch. *Starch/Staerke*, **30**, 73-78.
 [13] Buléon, A., Colonna, P., Planchot, V. and Ball, S. (1998) Starch granules: structure and biosynthesis. *Int. J. Biol. Macrom.*, **23**, 85-112.
 [14] Waigh, T.A., Donald, A.M., Heidelberg, F., Riekkel, C. and Gidley, M.J. (1999) Analysis of the native structure of starch granules with small-angle X-ray microfocus scattering. *Biopolymers*, **49**, 91-105.
 [15] Waigh, T.A., Hopkinson, I., Donald, A.M., Butler, M., Heidelberg, F. and Riekkel, C. (1997) Analysis of the native structure of starch granules with X-ray microfocus diffraction. *Macromolecules*, **30**, 3813-3812.
 [16] Oostergetel, G.T., and van Bruggen, E.F.J. (1989) On the Origin of a Low Angle Spacing in Starch. *Starch/Staerke*, **41**, 331-335.
 [17] Jenkins, P.J., Cameron, R.E. and Donald, A.M. (1993) A universal feature in the study of starch granules from different botanical sources. *Starch/Staerke*, **45**, 417-420.

[18] Buléon, A., Bizot, H., Delage, M.M., and Multon, J.L. (1982) Evolution of crystallinity and specific gravity of potato starch versus ad- and desorption. *Starch/Staerke*, **34**, 361-366.
 [19] Imberty, A., Buléon, A., Trans, V., and Pérez, S. (1991) Recent advances in knowledge of starch structure. *Starch/Staerke*, **43**, 375-384.
 [20] Blackwell, J. (1969) Structure of β -chitin or parallel chain systems of poly- β -(1-4)-N-acetyl-D-glucosamine. *Biopolymers*, **7**, 281-298.
 [21] Gardner, H.H. and Blackwell, J. (1975) Refinement of the structure of β -chitin. *Biopolymers*, **14**, 1581-1595.
 [22] Saito, Y., Okano, T., Gail, F., Chanzy, H. and Puteaux, J.L. (2000) Structural data on intra-crystalline swelling of β -chitin. *Int. J. of Biol. Macrom.*, **28**, 81-88.
 [23] Saito, Y., Kumagai, H., Wada, M. and Kuga, S. (2002) Thermally reversible hydration of β -chitin. *Bio-macromolecules*, **3**, 407-410.
 [24] Pollack, L., Tate, M.W., Darnton, N.C., Knight, J.B., Gruner, S.M., Eaton, W.A. and Austin, R.H. (1999) Compactness of the denatured state of a fast-folding protein measured by submillisecond small-angle x-ray scattering. *Proc. Natl. Acad. Sci. USA*, **96**, 10115-10117.
 [25] Pollack, L., Tate, M.W., Finnefrock, A.C., Kalidas, C., Trotter, S., Darnton, N.C., Lurio, L., Austin, R.H., Batt, C.A., Gruner, S.M. and Mochrie, S.G.J. (2001) Time resolved collapse of a folding protein observed with small angle X-ray scattering. *PRL*, **86**, 4962-4965.
 [26] Knight, J.B., Vishwanath, A., Brody, J.P. and Austin, R.H. (1998) Hydrodynamic focusing on a silicon chip: Mixing Nanoliters in Microseconds. *PRL*, **80**, 3863-3866.
 [27] Saito, Y., Okano, T., Gaill, J.L. and Chanzy, H. (1998) in *Advances in Chitin Science*, A. Domard, G.A.F. Roberts, and K.M. Varum, Editors Jacques Andre Publ.: Lyon, 507.
 [28] web page: www.proxitronic.de.